Solubility and Phase Behaviors of AOT Analogue Surfactants in 1,1,1,2-Tetrafluoroethane and Supercritical Carbon Dioxide

Zhao-Tie Liu,*,† Ling Liu,† Jin Wu,† Liping Song,† Ziwei Gao,† Wensheng Dong,† and Jian Lu‡

Key Laboratory for Macromolecular Science of Shaanxi Province, School of Chemistry & Materials Science, Shaanxi Normal University, Xi'an, 710062, People's Republic of China, and Xi'an Modern Chemistry Research Institute, Xi'an, 710065, People's Republic of China

A series of AOT (aerosol-OT) analogue surfactants (sodium salt of dibutyl-2-sulfosuccinate, sodium salt of dipentyl-2-sulfosuccinate, sodium salt of dihexyl-2-sulfosuccinate, and sodium salt of dioctyl-2-sulfosuccinate) were synthesized and characterized by ^{1}H NMR and elemental analysis. A static method coupled with gravimetric analysis is developed to measure the solubility of the surfactants in 1,1,1,2-tetrafluoroethane (HFC-134a) and supercritical CO_2 ($scCO_2$). The solubilities of the surfactants in HFC-134a and $scCO_2$ are affected by the temperature, pressure, and carbon atom number of the surfactant. The solubility of the same surfactant in HFC-134a solvent is approximately two times that in the most commonly used supercritical solvent CO_2. The pressure−temperature phase diagrams for water/HFC-134a microemulsions stabilized by the surfactants were determined using cloud-point measurements for a concentration range of the surfactant from (1.85×10^{-3} to 5.60×10^{-3}) M, temperature up to 338 K, and pressure up to 40 MPa in a high-pressure vessel. At a fixed temperature, the cloud-point pressure increased with increasing water-to-surfactant molar ratio (W_o). At a fixed W_o, the cloud-point pressure decreased with increasing temperature. The surfactant with the longest hydrocarbon chain has the highest cloud-point pressure even at lower surfactant concentrations.

Introduction

Supercritical carbon dioxide ($scCO_2$) is an attractive substitute for organic solvents since it has low toxicity, is nonflammable, and is cheap and readily available in large quantities.[1−5] With these advantages together with its unique properties as a supercritical fluid such as its adjustable solvent power, enhanced mass transfer characteristics, and low surface tension, $scCO_2$ has prompted extensive research to develop $scCO_2$-based processes.[6−10]

With growing interest in nanostructured materials, a number of techniques have been used for production of nanoparticles, such as gas evaporation,[11] sputtering,[12] coprecipitation,[13] sol−gel method, hydrothermal,[14] microemulsion,[15−17] etc. Water-in-oil (W/O) microemulsions have received great attention. A microemulsion is a thermodynamically stable system with at least three components: two immiscible components (generally water and oil) and a surfactant. Recent experiments[18,19] have been investigated for the use of carbon dioxide (CO_2) as a nonpolar solvent medium for formation of microemulsions.

Unfortunately, because CO_2 is a nonpolar solvent and has weak van der Waals forces, it is not suitable for dissolving polar substances, which has limited its application in the separation, reaction and material formation processes. Many supercritical fluids exhibit a low polarity, and many polar solutes are insoluble in them. Generally the more polar the fluid, the higher the critical temperature (T_c). Halogenated aliphatic compounds offer more polar solvation media but still have readily accessible critical constants. At present only a small number of such fluids[20,21] have been studied, including CF_3H and CCl_3F. Owing to their low toxicity and nonflammability, alternative hydrofluorocarbon (HFC) propellants would be desirable.[22]

Olsen and Tallman[23,24] were the first to use HFCs for electrochemical experiments in supercritical solvents. The solvent properties of 1,1,1,2-tetrafluoroethane (HFC-134a) have been investigated thoroughly as a function of temperature and pressure. This solvent was shown to be more polar than studied chlorofluorocarbons (CFCs), even though it has a relatively low critical temperature and pressure ($T_c = 374$ K, $P_c = 4.055$ MPa). Abbott et al.[25] also performed electrochemical measurements in HFC-134a and difluoromethane.

Tackson and Fulton[26] reported the properties of sodium bis-(2-ethylhexyl) sulfosuccinate (AOT) microemulsions formed in supercritical hydrochlorofluorocarbons (HCFCs), HFC, and fluorocarbons. They also reported extensively the phase behavior of AOT and didodecyldimethylammonium bromide microemulsions formed in supercritical chlorodifluoromethane (R22). Microemulsions formed in R22 were demonstrated to have a strongly density-dependent maximum molar water-to-surfactant ratio (W_o).

Water-in-fluorocarbon emulsion formation in the HFCs gases 1,1,1,2,3,3,3-heptafluoropropane (R227) and HFC-134a has recently been investigated by Butz et al.[27] using perfluoroalkylated dimorpholinophosphate ($F_8H_{11}DMP$) as the surfactant. Water solubilization by anionic perfluorinated surfactants has been examined in the condensed phase of the HFC-134a in the temperature range (288 to 328) K and under a pressure of 50 MPa.[28]

Johnston et al.[29] discovered that an ammonium carboxylate perfluoropolyether [$CF_3O(CF_2CF(CF_3)OCF_2COONH_4$, PEPF] surfactant could support a microemulsion in $scCO_2$. A promising recent development in this field has been the demonstration of the ability of a fluorinated analogue of AOT.[30]

* Corresponding author. Fax: +86 29 85303682. E-mail: ztliu@snnu.edu.cn.
† Shaanxi Normal University.
‡ Xi'an Modern Chemistry Research Institute.

10.1021/je060152v CCC: $33.50
Published on Web 10/19/2006

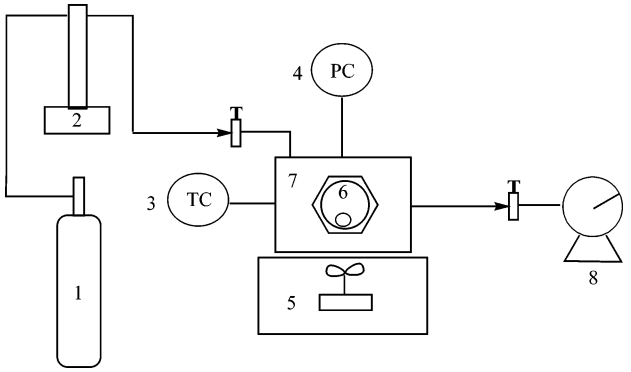

Figure 1. Schematic diagram for solubility and phase diagram measurements: 1, steel cylinder; 2, syringe pump; 3, thermocouple assembly; 4, pressure transducer; 5, magnetic stirrer; 6, glass vial; 7, high-pressure vessel; 8, wet-type gas meter.

The current work describes the solubilities and pressure-temperature phase diagrams for W/HFC-134a (water/HFC-134a) microemulsions stabilized by the surfactants using cloud-point measurements for a surfactant concentration of (1.85×10^{-3} to 5.60×10^{-3}) M, temperature up to 338 K, and pressure up to 40 MPa. These phase diagrams are important to the formation of nanoparticales in our further studies.

Experimental Section

Materials and Instruments. Maleic anhydride (99.5 %), *p*-toluenesulfonic acid monohydrate (99 %), 1,4-dioxane (99 %), sodium hydrogen sulfite (SO_2, 65.0 %) and *n*-hexanol (99.0 %) were obtained from the Sinopharm Group Chemical Reagent Co. Toluene (99.5 %), *n*-pentanone (98 %), *n*-octanol (99.5 %), and sodium hydroxide (96.0 %) were obtained from the Xi'an Chemical Reagent Factory. *n*-Butanol (99.0 %) was obtained from the Tianjin No. 3 Chemical Reagent Factory. CO_2 was obtained from the Xi'an Yatai Liquid Gas Co., and 1,1,1,2-tetrafluoroethane (HFC-134a) (99.9 %) was obtained from the Xi'an Jinzhu Modern Chemical Industry Co., Ltd. The chemical reagents used in this study were of analytical pure grade. All the chemicals were used directly without further purification.

A schematic diagram of the experimental setup for solubility measurements is given in Figure 1. The high-pressure vessel (Beijing, Sihe Chuangzhi Keji Corporation, SF-400) with a maximum pressure of 40 MPa, a maximum temperature of 353 K, and an internal volume of 60 cm^3 was equipped with two sapphire windows with a diameter of 25 mm and a thickness of 20 mm. The windows were sealed on both sides with poly(ether−ether−ketone) (PEEK) seals. The high-pressure vessel was also fitted with a thermocouple assembly, a pressure transducer, and a rupture disk assembly. The vessel rests on a magnetic stirrer, and fluid is introduced into the pressure vessel using a syringe pump (model 260D, ISCO).

The ^{1}H NMR spectra were recorded on a superconducting Fourier digital NMR spectrometer (Bruker, AVANCF 300 MHZ). The elemental analysis of the samples was performed by an elemental analyzer (Germany, Vario EL III) with a variation of ± 0.5 %.

Synthesis of Surfactants. The modified synthesis procedures of surfactants were conducted according to the methods given by Liu and Erkey.[31] The synthesis procedure of the surfactants (sodium salt of dibutyl-2-sulfosuccinate, DBSS; sodium salt of dipentyl-2-sulfosuccinate, DPSS; sodium salt of dihexyl-2-sulfosuccinate, DHSS; and sodium salt of dioctyl-2-sulfosuccinate, DOSS) has two main steps: esterification and sulfonation reaction.

A mixture of maleic anhydride, *n*-pentanone (or *n*-octanol, *n*-butanol, *n*-hexanol), and *p*-toluenesulfonic acid monohydrate as the catalyst in a flask was refluxed under stirring at 398 K for 2 h. The water created in this reaction was collected in a trap. The yield of this esterification reaction was approximately 80 %.

Esterifiable product was neutralized to the pH of 7 using an aqueous sodium hydroxide (30 %) solution. Floc was observed in the system. Then an aqueous sodium hydrogen sulfite and ethanol as cosolvent were added into the system. The mixture was refluxed under stirring at 393 K for (3 to 4) h. A little of the product was then taken out into water and stirred to determine the reaction degree. The reaction was stopped if no oily matter floated on the water surface and the pH of the reaction system was (7 to 8). After reacting, the viscous liquid was created in the flask. This liquid was placed in a dryer to remove water in the system. The solid obtained was then dissolved in anhydrous alcohol and recrystallized. A white solid was obtained after drying at 323 K under vacuum overnight. The surfactants were characterized by ^{1}H NMR spectroscopy and elemental analysis as follows.

Sodium Salt of Dioctyl-2-sulfosuccinate. $CH_3^a(CH_2)_5^bCH_2^c$-$CH_2^dOOCCH_2^eCH^f(SO_3Na)COOCH_2^gCH_2^h(CH_2)_5CH_3^j$ (yield, 86.6 %). ^{1}H NMR ($CDCl_3$, δ): 0.880 (a and j, t, J = 6.75 Hz, 6H), 1.272 (b and i, m, J = 12.84 Hz, 20H), 1.586 (c and h, m, J = 5.76 Hz, 4H), 3.135−3.166 (e, m, J = 4.57 Hz, 2H), 4.024 (d, t, J = 6.87 Hz, 2H), 4.131−4.175 (g, m, J = 6.51 Hz, 2H), 4.269−4.317 (f, m, J = 4.04, 1H). Anal. Calcd for C, 54.03; S, 7.21; H, 8.39. Found: C, 54.97; S, 6.69; H, 8.33.

Sodium Salt of Dipentyl-2-sulfosuccinate. $CH_3^a(CH_2)_2^bCH_2^c$-$CH_2^dOOCCH_2^eCH^f(SO_3Na)COOCH_2^gCH_2^h(CH_2)_2^iCH_3^j$ (yield, 95.1 %). ^{1}H NMR ($CDCl_3$, δ): 0.908−0.873 (a and j, t, J = 3.70 Hz, 6H), 1.300−1.349 (b and i, m, J = 3.09 Hz, 8H), 1.673−1.550 (c and h, m, J = 6.89 Hz, 4H), 3.228−3.078 (e, m, J = 11.76 Hz, 2H), 4.035 (d, t, J = 6.84 Hz, 2H), 4.140−4.179 (g, m, J = 5.05 Hz, 2H), 4.262−4.311 (f, m, J = 4.95 Hz, 1H). Anal. Calcd for C, 46.65; S, 8.90; H, 6.99. Found: C, 46.14; S, 8.42; H, 6.71.

Sodium Salt of Dibutyl-2-sulfosuccinate. $CH_3^aCH_2^bCH_2^c$-$CH_2^dOOCCH_2^eCH^f(SO_3Na)COOCH_2^gCH_2^hCH_2^iCH_3^j$ (yield, 90.4 %). ^{1}H NMR ($CDCl_3$, δ): 0.93 (a and j, t, J = 2.96 Hz, 6H), 1.36 (b and i, t, J = 7.68 Hz, 4H), 1.58 (c and h, t, J = 7.55 Hz, 4H), 3.18 (e, t, J = 9.64 Hz, 2H), 4.05 (d, t, J = 6.73 Hz, 2H), 4.18 (g, t, J = 6.56 Hz, 2H), 4.33 (f, t, J = 5.12 Hz, 1H). Anal. Calcd for C, 43.37; S, 9.65; H, 6.37. Found: C, 43.31; S, 10.07; H, 6.41.

Sodium Salt of Dihexyl-2-sulfosuccinate. $CH_3^a(CH_2)_3^bCH_2^c$-$CH_2^dOOCCH_2^eCH^f(SO_3Na)COOCH_2^gCH_2^h(CH_2)_3^iCH_3^j$ (yield, 84.7 %). ^{1}H NMR ($CDCl_3$, δ): 0.90 (a and j, t, J = 4.59 Hz, 6H), 1.29 (b and i, t, J = 1.38 Hz, 8H), 1.59 (c and h, t, J = 6.87 Hz, 4H), 3.15 (e, t, J = 9.33 Hz, 2H), 4.05 (d, t, J = 6.87 Hz, 2H), 4.14 (g, t, J = 6.60 Hz, 2H), 4.33 (f, t, J = 5.16 Hz, 1H). Anal. Calcd for C, 49.47; S, 8.25; H, 7.52. Found: C, 49.57; S, 8.22; H, 7.41.

Measurements of Solubility. For each experiment, an excess amount of solute and a small magnetic stirring bar was placed in a 25 mm × 25 mm (12 mL) glass vial that was then capped with a coarse filter paper attached to the vial with Teflon tape. The sample vial was then weighed and placed inside the pressure vessel.

The vessel was sealed and heated to the desired temperature by a heater via a machined internal heating rod. Once the test temperature was reached, stirring was initiated, and the vessel was slowly filled with fluid until the desired pressure was

Table 1. Mass of Solute Lost from the Vial at Different Time (*t*) for DPSS in HFC-134a at 308 K and under 16 MPa[a]

T/K	*P*/MPa	*t*/h	*m*/g
308	25	5	0.0357
		9	0.0366
		13	0.0375
		16	0.0378
		20	0.0382
		24	0.0381
		28	0.0382

[a] *m*, amount dissolved of surfactant.

achieved. After sufficient time (usually more than 20 h as explained in the Results and Discussion section) was allowed for equilibration of fluid/solute solution, the vessel was depressurized and opened. The vial was removed, wiped with a clean tissue, dried, and reweighed. The solubility of the solute is then given by the equation as follows:

$$\text{solubility (wt/vol)} = \frac{W_1 - W_2}{V_1 - V_2}$$

where W_1 and W_2 are the initial and final measured mass of solute in the vial, V_1 is the volume of the high-pressure vessel, and V_2 is the volume of vial. This equation incorporates a correction factor that accounts for precipitation of the solute in the fluid phase in the vial. The volume of the vessel in this equation is the volume accessible to the fluid phase, which was determined to be 48 mL.

Measurement Pressure−Temperature Phase Diagrams of Surfactants. The pressure−temperature (*P*−*T*) phase diagrams for W/HFC-134a microemulsions stabilized by the surfactants were determined using cloud-point measurements.[31,32] The macroscopic phase behavior of the surfactant aggregates in HFC-134a was investigated using a high-pressure vessel. In a typical experiment, a certain amount of surfactant and water and a magnetic stir bar were placed in the vessel, which was then sealed. The vessel was then placed on a magnetic stirrer and heated to the desired temperature. The vessel was charged very slowly with HFC-134a from a syringe pump (ISCO, 260D) equipped with a cooling jacket. When an optically transparent single-phase solution was obtained, the pump was stopped. Subsequently, the vessel was slowly depressurized until the cloud point was reached. The temperature was controlled during each experiment with a variation of ± 0.5 °C. The pressure was measured using a pressure transducer (Beijing, Zhengkai, MCY-B) and was controlled during each experiment with a variation of ± 0.01 MPa.

Results and Discussion

Measurements of Solubility. A static method coupled with gravimetric analysis was developed for measuring the solubility of the surfactants in $scCO_2$ and HFC-134a.[33] In order to obtain accurate solubility of surfactant and shorten the experiment time, the first set of experiments was conducted to determine the time necessary for achieving equilibrium and the accuracy of solubility in this system. The data of the mass of solute lost from the vial at different times was listed in Table 1 for DPSS in HFC-134a at 308 K and under 16 MPa. The fluid phase became saturated with DPSS after about 20 h. The solubility of DPSS in $scCO_2$ was obtained at a fixed pressure with changing temperature as shown in Table 2.

Table 3 reveals that the solubility of DPSS in $scCO_2$ increases with an increase in pressure at a constant temperature, with the influence of pressure on the solubility being more pronounced

Table 2. Solubility of DPSS in $scCO_2$ with Increasing of Temperature under a Pressure of 25 MPa[a]

P/MPa	*T*/K	*m*/g	S ($\times 10^{-4}$)/g·mL^{-1}
25	308	0.0161	3.354
	318	0.0372	7.750
	328	0.0515	10.73
	338	0.0549	11.44

[a] *m*, amount dissolved of surfactant; *S*, solubility.

Table 3. Solubility of DPSS in $scCO_2$ with Increasing of Pressure at a Temperature of 318 K[a]

T/K	*P*/MPa	*m*/g	S ($\times 10^{-4}$)/g·mL^{-1}
318	15	0.0455	9.479
	20	0.0472	9.833
	25	0.0500	10.42
	30	0.0597	12.44
	35	0.0642	13.38

[a] *m*, amount dissolved of surfactant; *S*, solubility.

at higher temperature. Under lower pressure, the increasing trend of solubility with an increase in pressure is slow, while under a higher pressure, the increasing trend is fast. Pressure is the main influencing factor on the density of the supercritical fluid: when the pressure is higher, the density of the supercritical fluid is greater. The solubility of solute in the supercritical fluid is greatly related to the density and increases with an increase in density. So the solubility of the surfactant increases with an increase in pressure. This is in accord with conventional wisdom stating that the density of a supercritical fluid must increase in order to increase the solubility and extraction efficiency.[34] Considering the thermodynamic view, at the same temperature, on the basis of the Hildebrandt flexibility formula $\Delta H_M V(\delta_1 - \delta_2)$, if the solubility parameter of a supercritical fluid solvent δ_1 and solubility parameter of a solute δ_2 are closer, the mixture heat ΔH_M is smaller, and the two compounds can dissolve each other.

The solubility of DPSS in $scCO_2$ increases with an increase in temperature. The effect of temperature on solubility is complex. The crossover of solubility isotherms occurs when pressure is used as a variable. The phenomenon is a consequence of two competitive effects: the density of $scCO_2$ and the vapor pressure. As the temperature increases, the vapor pressure increases too, which enhances the solubility. But the density and CO_2 solvent power decrease, which results in a decrease in solubility. At pressures above the crossover region, the solubility increases with an increase in both pressure and temperature while, below this point, the solubility increases with an increase in pressure but decreases with an increase in temperature. At lower pressure, the fluid density is lowered by a small increase in temperature. Since the density effect is predominant in this region, the solubility will decrease with an increase in temperature. However, at higher pressure the fluid density is less dependent on temperature so that the observed increase in solubility with an increase in temperature could be primarily due to other factors, especially the higher vapor pressure of solid samples.[35,36] While fixing the pressure at 25 MPa, which is above the crossover region, so an increase in solubility with an increase of temperature was observed.

The solubility results for DPSS in HFC-134a at a fixed temperature are shown in Table 4. The solubility of DPSS in HFC-134a increases with an increase in pressure. The solubility results for DPSS in HFC-134a at a fixed pressure are listed in Table 5. The solubility of DPSS in HFC-134a increases with an increase in temperature. The solubility of DPSS in HFC-

Table 4. Solubility of DPSS in HFC-134a with Increasing of Pressure at a Temperature of 318 K[a]

T/K	*P*/MPa	*m*/g	*S* ($\times 10^{-3}$)/g·mL^{-1}
318	16.5	0.0435	0.9063
	20.2	0.0604	1.2583
	25.0	0.0702	1.4625
	30.0	0.0898	1.8708
	33.0	0.1139	2.3729

[a] *m*, amount dissolved of surfactant; *S*, solubility.

Table 5. Solubility of DPSS in HFC-134a with Increasing of Temperature under a Pressure of 25 MPa[a]

P/MPa	*T*/K	*m*/g	*S* ($\times 10^{-4}$)/g·mL^{-1}
25	308	0.0341	7.104
	318	0.0702	14.63
	328	0.1124	23.42
	338	0.2467	51.40

[a] *m*, amount dissolved of surfactant; *S*, solubility.

Table 6. Comparison of Solubility of DPSS in HFC-134a and scCO$_2$ with Increasing of Pressure and at a Temperature of 318 K[a]

		m/g		*S* ($\times 10^{-4}$)/g·mL^{-1}	
T/K	*P*/MPa	CO_2	HFC-134a	CO_2	HFC-134a
318	15	0.0455	0.0435	9.479	9.062
	20	0.0472	0.0604	9.833	12.58
	25	0.0500	0.0702	10.42	14.63
	30	0.0597	0.0898	12.49	18.70
	35	0.0642	0.1139	13.38	23.73

[a] *m*, amount dissolved of surfactant; *S*, solubility.

Table 7. Comparison of Solubility of DPSS in HFC-134a and scCO$_2$ with Increasing of Temperature and Under a Pressure of 25 MPa[a]

		m/g		*S* ($\times 10^{-4}$)/g·mL^{-1}	
P/MPa	*T*/K	CO_2	HFC-134a	CO_2	HFC-134a
25	308	0.0161	0.0341	3.354	7.104
	318	0.0372	0.0702	7.750	14.63
	328	0.0515	0.1124	10.73	23.42
	338	0.0549	0.2467	11.49	51.40

[a] *m*, amount dissolved of surfactant; *S*, solubility.

134a is affected by pressure and temperature as shown in Table 4 and Table 5, and the trend of solubility is consistent with that in scCO$_2$.

The theory of solubility parameters can qualitatively explain the effect of pressure and temperature on the solubility of a solute. When the solubility parameters of the solute and solvent are closer, the solubility increases. The solubility parameter of the solute is related to the property of the solute and the temperature. Generally, the solubility parameter of a solute decreases with an increase in temperature. When the pressure increases while the temperature keeps constant, the solubility parameter of solute is a constant.

The solubility of the same surfactant in HFC solvent is approximately two times that in the most commonly used scCO$_2$ as given in Table 6 and Table 7, because CO_2 is a nonpolar solvent and has weak van der Waals forces, so it is not suitable for dissolving polar substances in this medium. The increase in solubility in the HFC-134a medium is to some extent what would be expected for a polar solute in this more polar solvent. For these systems, a dipole−dipole interaction between the polar solute and HFC-134a exists, which would tend to enhance solubility relative to that with the dipole−quadrupole interaction present with the polar solutes and the scCO$_2$ system.[37]

Table 8. Solubility of Different Surfactants in HFC-134a under 25 MPa and at 318 K[a]

surfactant	*m*/g	*S* ($\times 10^{-4}$)/g·mL^{-1}
DBSS	0.1101	22.94
DPSS	0.0702	14.63
DHSS	0.0439	9.125
DOSS	0.0270	5.625

[a] *m*, amount dissolved of surfactant; *S*, solubility.

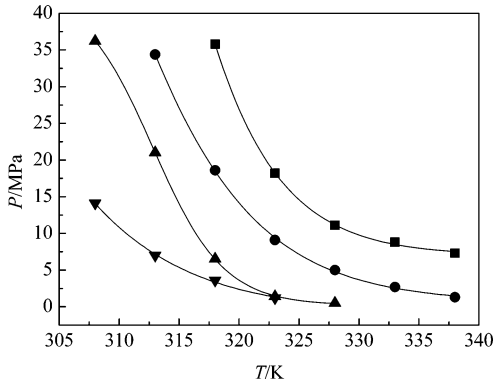

Figure 2. Effect of W_o on $P-T$ phase diagram for W/HFC-134a microemulsions supported by DPSS at [surfactant] = 0.00185 M: ■, W_o = 30; ●, W_o = 25; ▲, W_o = 20; ▼, W_o = 15.

The solubility results for different surfactants in HFC-134a at the same temperature and pressure are listed in Table 8. The solubility of sodium salt sulfosuccinate in HFC-134a decreases with an increase of the number of carbon atoms under the same conditions, which indicates the existence of hydrocarbon chain length controlling the solubility of surfactant in HCF-134a. Generally, the molecular weight of the compound is higher, its solubility in the fluid is lower. The surfactant with the longer hydrocarbon chain length has a stronger polarity. HCF-134a is a polar solvent, so the solubility of the surfactant with the longer hydrocarbon chain length is higher than that with a shorter hydrocarbon chain length.

A static method coupled with gravimetric analysis was developed for measuring the solubility of solids in scCO$_2$. The appealing feature of this technique is its simplicity, and it requires no specialized equipment other than a suitable pressure cell. The technique can, in principle, be easily extended to the measurement of solubilities of mixtures of solids in scCO$_2$ if the composition of the remaining mixture in the vial can be determined by a suitable chemical analysis such as GC, HPLC, or infrared or UV−vis spectroscopy. Preliminary mass-transfer calculations of this technique indicate that the major resistance to mass transfer was the filter paper. The time necessary for achieving equilibrium can probably be reduced by using a thinner membrane to cap the sample vial.[33]

Measurement Pressure−Temperature Phase Diagrams of Surfactants. The $P-T$ phase stability diagram for W/HFC-134a microemulsions supported by the DPSS surfactant at different W_o values is shown in Figure 2 and Figure 3. The cloud-point pressures increase with increasing W_o at a fixed temperature. This behavior is indicative of swelling of micelles with added water, which in turn strengthens attractive micelle−micelle interactions. Thus, higher pressures are required to strengthen tail−solvent interactions to prevent phase separation. While the cloud-point pressures decrease with increasing temperature at a fixed W_o. This result is different from that in scCO$_2$. Perhaps because there is a dipole−quadrupole interaction present in the polar solute and scCO$_2$ system, while there is a dipole−dipole interaction between the polar solute and HFC-134a. This

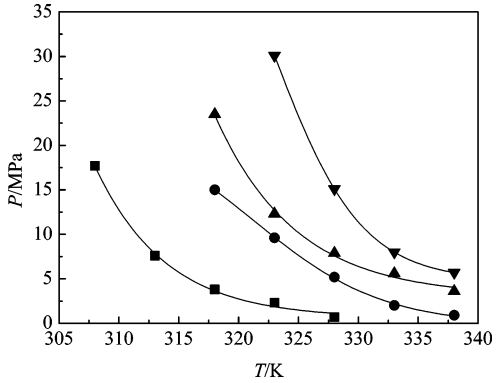

Figure 3. Effect of W_o on $P-T$ phase diagram for W/HFC-134a microemulsions supported by DPSS at [surfactant] = 0.0037 M: ▼, W_o = 25; ▲, W_o = 20; ●, W_o = 15; ■, W_o = 10.

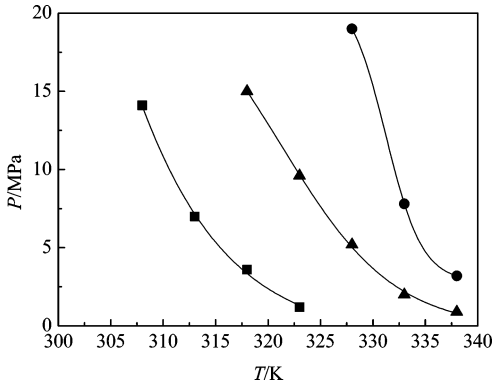

Figure 4. Effect of surfactant concentration on $P-T$ phase diagram for W/HFC-134a microemulsions supported by DPSS at W_o = 15: ●, 0.0056 M; ▲, 0.0037 M; ■, 0.00185 M.

interaction is likely to influence the phase behaviors of the surfactant in fluids.

The $P-T$ phase diagram at W_o = 15 for different DPSS concentrations is shown in Figure 4. Without any added water, the surfactant does not dissolve completely under these concentrations, resulting in a separate solid phase at the bottom of the vessel. However, a cloud point can still be reached by reducing pressure, indicating that a substantial amount of surfactant still dissolves in HFC-134a. The addition of water stabilizes the system, and an optically transparent solution can be obtained. As the surfactant concentrations increases from (1.85×10^{-3} to 5.60×10^{-3}) M, there is an appreciable increase in cloud-point pressure. When the surfactant concentrations increase from (1.85×10^{-3} to 5.60×10^{-3}) M, the amount of micelles per unit volume increases gradually, and the micelle−micelle distance decreases, which strengthens attractive micelle−micelle interactions. Thus, higher pressures are required to strengthen tail-solvent interactions to prevent phase separation.

The $P-T$ phase diagram for W/HFC-134a microemulsions stabilized by the two surfactants (DPSS and DBSS) is given in Figure 5. The surfactant concentrations for DPSS and DBSS are 0.0037 M with W_o = 20. However, DHSS and DOSS cannot form microemulsions in HFC-134a because their solubilities in HFC-134a are smaller. Microemulsions cannot be formed at a significantly lower surfactant concentration, indicating that hydrocarbon chain length affects the cloud pressure greatly. The longer hydrocarbon chain, the higher cloud pressure the surfactant has, as reported by Bousquet et al.[22] The fact that the surfactant with the longest hydrocarbon chain has the highest cloud-point pressure even at lower surfactant concentrations is very interesting. The HFC-134a-philicity of the tail group must

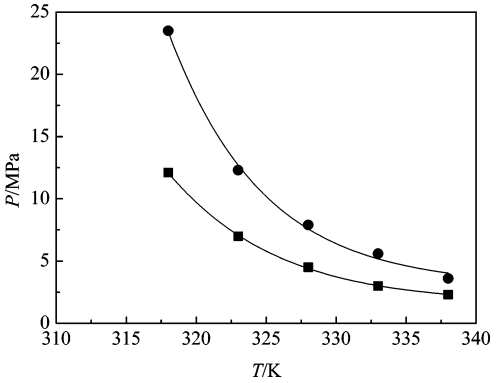

Figure 5. Comparison of $P-T$ phase diagram for W/HFC-134a microemulsions supported by two different surfactants DBSS and DPSS at 0.0037 M and W_o = 20: ■, DBSS; ●, DPSS.

be decreasing with an increasing length of the hydrocarbon chain, and the tail−solvent interactions are too weak to compensate for attractive micelle−micelle interactions. This is in accordance with previous findings on CO_2-philic chelating agents[38] and homogeneous catalysts[39] that small fluoroalkyl chains are as effective as long fluoroalkyl or fluoropolymer chains for solubility enhancement in $scCO_2$.

Conclusion

A series of AOT analogue surfactants were synthesized and characterized. A static method coupled with gravimetric analysis was developed for measuring the solubility of surfactants in $scCO_2$ and HFC-134a fluids. The solubility of a particular solute was affected by pressure, temperature, solvent polarity, and the number of carbon atoms of surfactant. The solubility of polar solutes in the HFC-134a medium was found to be much higher than that in the most commonly used supercritical solvent CO_2. The pressure−temperature phase diagrams for W/HFC-134a microemulsions stabilized by the surfactants were determined using cloud-point measurements. The phase behaviors of different surfactants as a function of temperature, pressure, and W_o are obtained in this work, which are useful in formation of nanoparticles synthesis in these microemulsions.

Literature Cited

(1) Müller, M.; Meier, U.; Kessler, A.; Mazzotti, M. Experimental study of the effect of process parameters in the recrystallization of an organic compound using compressed carbon dioxide as antisolvent. *Ind. Eng. Chem. Res.* **2000**, *39*, 2260−2268.
(2) Yates, M. Z.; Birnbaum, E. R.; McCleskey, T. M. Colored polymer microparticles through carbon dioxide-assisted dyeing. *Langmuir* **2000**, *16*, 4757−4760.
(3) Kendall, J. L.; Canelas, D. A.; Young, J. L.; DeSimone, J. M. Polymerizations in supercritical carbon dioxide. *Chem. Rev.* **1999**, *99*, 543−564.
(4) Zhang, J. L.; Han, B. X.; Liu, J. C.; Zhang, X. G.; Yang, G. Y.; Zhao, H. Z. Size tailoring of ZnS nanoparticles synthesized in reverse micelles and recovered by compressed CO_2. *J. Supercrit. Fluids* **2004**, *30*, 89−95.
(5) Shah, P. S.; Husain, S.; Johnston, P. K.; Korgel, B. A. Nanocrystal arrested precipitation in supercritical carbon dioxide. *J. Phys. Chem. B.* **2001**, *105*, 9433−9440.
(6) Chattopadhyay, P.; Gupta, R. B. Supercritical CO_2-based production of fullerene nanoparticles. *Ind. Eng. Chem. Res.* **2000**, *39*, 2281−2289.
(7) Wakayama, H.; Itahara, H.; Tatsuda, N.; Inagaki, S.; Fukushima, Y. Nanoporous metal oxides synthesized by the nanoscale casting process using supercritical fluids. *Chem. Mater.* **2001**, *13*, 2392−2396.
(8) Liu, S.; Jonathan, V. M.; Weaver, M. S.; Armes, S. P. Synthesis of pH-responsive shell cross-linked micelles and their use as nanoreactors for the preparation of gold nanoparticles. *Langmuir* **2002**, *18*, 8350−8357.
(9) Chen, D. H.; Wu, S. H. Synthesis of nickel nanoparticles in water-in-oil microemulsions. *Chem. Mater.* **2000**, *12*, 1354−1360.

(10) Ohde, H.; Ohde, M.; Bailey, F.; Kim, H.; Wai, C. M. Water-in-CO_2 microemulsions as nanoreactors for synthesizing CdS and ZnS nanoparticles in supercritical CO_2. *Nano. Lett.* **2002**, *2*, 721−724.
(11) Kodama, S.; Kido, O.; Suzuki, H.; Saito, Y.; Kaito, C. Characterization of nanoscale $BaTiO_3$ ultrafine particles prepared by gas evaporation method. *J. Cryst. Growth* **2005**, *282*, 60−65.
(12) Sun, C. L.; Chen, L. C.; Su, M. C.; Hong, L. S.; Chyan, O.; Hsu, C. Y.; Chen, K. H.; Chang, T. F.; Chang, L. Ultrafine platinum nanoparticles uniformly dispersed on arrayed CN_x nanotubes with high electrochemical activity. *Chem. Mater.* **2005**, *17*, 3749−3754.
(13) Tang, Z. X.; Sorensen, C. M.; Klabunde, K. J.; Hadjipanayis, G. C. Preparation of manganese ferrite fine particles from aqueous solution. *J. Colloid Interface Sci.* **1991**, *146*, 38−52.
(14) Lou, X. W.; Zeng, H. C. Hydrothermal synthesis of -MoO_3 nanorods via acidification of ammonium heptamolybdate tetrahydrate. *Chem. Mater.* **2002**, *14*, 4880−4880.
(15) Gao, D.; He, R.; Carraro, C.; Howe, R. T.; Yang, P.; Maboudian, R. Selective growth of Si nanowire arrays via galvanic displacement processes in water-in-oil microemulsions. *J. Am. Chem. Soc.* **2005**, *127* (13), 4574−4575.
(16) Yin, Z.; Sakamoto, Y.; Yu, J.; Sun, S.; Terasaki, O.; Xu, R. Microemulsion-based synthesis of titanium phosphate nanotubes via amine extraction system. *J. Am. Chem. Soc.* **2004**, *126*, 8882−8883.
(17) Ohde, H.; Wai, C. M.; Kim, H.; Kim, J.; Ohde, M. Hydrogenation of olefins in supercritical CO_2 catalyzed by palladium nanoparticles in a water-in-CO_2 microemulsion. *J. Am. Chem. Soc*. **2002**, *124*, 4540−4541.
(18) Sagisaka, M.; Yoda, S.; Takebayashi, Y.; Otake, K.; Kitiyanan, B.; Kondo, Y.; Yoshino, N.; Takebayashi, K.; Sakai, H.; Abe, M. Preparation of a W/scCO_2 microemulsion using fluorinated surfactants. *Langmuir* **2003**, *19*, 220−225.
(19) Hoefling, T. A.; Enick, R. M.; Beckman, E. J. Microemuisions in near-critical and supercritical CO_2. *J. Phys. Chem.* **1991**, *95*, 7127−7129.
(20) Yonker, C. R.; Frye, S. L.; Kalkwarf, D. R.; Smith, R. D. Character-lzatlon of supercritical fluid solvents using solvatochromic shifts. *J. Phys. Chem.* **1986**, *90*, 3022−3026.
(21) Kajimoto, O.; Futakami, M.; Kobayashi, T.; Yamasaki, K. Charge-transfer-state formation in supercritical fluid: (*N*,*N*-dimethylamino) benzonitrile in CF_3H. *J. Phys. Chem.* **1988**, *92*, 1347−1352.
(22) Bousquet, J.; Cantini, L. Clinical studies in asthmatics with a new non-extra fine HFA formulation of beclometasone dipropionate, *Respir. Med.* **2002**, *96*, S17−S27.
(23) Olsen, S. A.; Tallman, D. E. Voltammetry of ferrocene in subcritical and supercritical chlorodifluoromethane. *Anal. Chem.* **1994**, *66*, 503−509.
(24) Olsen, S. A.; Tallman, D. E. Conductivity and voltammetry in liquid and supercritical halogenated solvents. *Anal. Chem.* **1996**, *68*, 2054−2061.
(25) Abbott, A. P.; Eardley, C. A.; Harper, J. C.; Hop, E. G. Electrochemical investigations in liquid and supercritical 1,1,1,2-tetrafluoroethane (HFC-134a) and difluoromethane (HFC 32). *J. Electroanal. Chem.* **1998,** *457*, 1−4.
(26) Tackson, K.; Fulton, J. L. Microemulsions in supercritical hydrochlorofluorocarbons. *Langmuir* **1996**, *12*, 5289−5295.
(27) Butz, N.; Porte, C.; Courrier, H.; Krafft, M. P.; Vandamme, T. F. Reverse water-in-fluorocarbon emulsions for use in pressurized metered-dose inhalers containing hydrofluoroalkane propellants. *Int. J. Pharm.* **2002**, *238*, 257−269.
(28) Eastoe, J.; Thorpe, A. M.; Eastone, J.; Dupont, A.; Heenan, R. K. Microemulsion formation in 1,1,1,2-tetrafluoroethane (R134a). *Langmuir* **2003**, *19*, 8715−8720.
(29) Johnston, K. P.; Harrison, K. L.; Clarke, M. J.; Howdle, S. M.; Heitz, M. P.; Bright, F. V.; Carlier, C.; Randolph, T. W. Water-in-carbon dioxide microemulsions: an environment for hydrophiles including proteins. *Science* **1996**, *271*, 624−626.
(30) Sagisaka, M.; Yoda, S.; Takebayashi, Y.; Otake, K.; Kondo, Y.; Yoshino, N.; Sakai, H.; Abe, M. Effects of CO_2-philic tail structure on phase behavior of fluorinated aerosol-OT analogue surfactant/water/supercritical CO_2 systems. *Langmuir* **2003**, *19*, 8161−8167.
(31) Liu, Z. T.; Erkey, C. Water in carbon dioxide microemulsions with fluorinated analogues of AOT. *Langmuir* **2001**, *17*, 274−277.
(32) Dong, X.; Erkey, C.; Dai, H. J.; Li, H. C.; Cochran, H. D.; Lin, J. S. Phase behavior and micelle size of an aqueous microdispersion in supercritical CO_2 with a novel surfactant. *Ind. Eng. Chem. Res.* **2002**, *41*, 1038−1042.
(33) Sherman, G.; Shenoy, S.; Weiss, R. A.; Erkey, C. A static method coupled with gravimetric analysis for the determination of solubilities of solids in supercritical carbon dioxide. *Ind. Eng. Chem. Res.* **2000**, *39*, 846−848.
(34) Miller, D. J.; Hawthorne, S. B. Determination of solubilities of organic solutes in supercritical CO_2 by on-line flame ionization detection. *Anal. Chem.* **1995**, *67*, 273−279.
(35) Xing, H.; Yang, Y.; Su, B.; Huang, M.; Ren, Q. Solubility of artemisinin in supercritical carbon dioxide. *J. Chem. Eng. Data* **2003**, *48*, 330−332.
(36) Khosravi-Darani, K.; Vasheghani-Farahani, E.; Yamini, Y.; Bahrami-far, N. Solubility of poly(α-hydroxybutyrate) in supercritical carbon dioxide. *J. Chem. Eng. Data* **2003**, *48*, 860−863.
(37) Abbott, A. P.; Corr, S.; Durling, N. E.; Hope, E. G. Solubility of substituted aromatic hydrocarbons in supercritical difluoromethane. *J. Chem. Eng. Data* **2002**, *47*, 900−905.
(38) Erkey, C. Supercritical carbon dioxide extraction of metals from aqueous solutions: a review. *J. Supercrit. Fluids* **2000**, *17*, 259−287.
(39) Palo, D. R.; Erkey, C. Effect of ligand modification on rhodium-catalyzed homogeneous hydroformylation in supercritical carbon dioxide. *Organometallics* **2000**, *19*, 81−86.

Received for review April 6, 2006. Accepted September 16, 2006. Acknowledgment is made to the National Natural Science Foundation of China (NSFC) (20473051) and the Special Project of National Grand Fundamental Research Pre-973 Program of China (Program/Grant 2004CCA00700) for the support of this research. We also appreciate the support provided by the Natural Science Foundation of Shaanxi Province (2004B12).

JE060152V